

# A SUBMILLIMETER GALAXY ILLUMINATING ITS CIRCUMGALACTIC MEDIUM: LY $\alpha$ SCATTERING IN A COLD, CLUMPY OUTFLOW

J. E. GEACH<sup>1</sup>, R. G. BOWER<sup>2</sup>, D. M. ALEXANDER<sup>2</sup>, A. W. BLAIN<sup>3</sup>, M. BREMER<sup>4</sup>, E. L. CHAPIN<sup>5</sup>, S. C. CHAPMAN<sup>6</sup>,  
D. L. CLEMENTS<sup>7</sup>, K. E. K. COPPIN<sup>1</sup>, J. S. DUNLOP<sup>8</sup>, D. FARRAH<sup>9</sup>, T. JENNESS<sup>10,11</sup>, M. P. KOPROWSKI<sup>8</sup>, M. J. MICHAŁOWSKI<sup>8</sup>,  
E. I. ROBSON<sup>12</sup>, D. SCOTT<sup>13</sup>, D. J. B. SMITH<sup>1</sup>, M. SPAANS<sup>14</sup>, A. M. SWINBANK<sup>2</sup>, P. VAN DER WERF<sup>15</sup>

*Draft version February 27, 2014*

## ABSTRACT

We report the detection at 850  $\mu\text{m}$  of the central source in SSA22-LAB1, the archetypal ‘Lyman- $\alpha$  Blob’ (LAB), a 100 kpc-scale radio-quiet emission-line nebula at  $z = 3.1$ . The flux density of the source,  $S_{850} = 4.6 \pm 1.1$  mJy implies the presence of a galaxy, or group of galaxies, with a total luminosity of  $L_{\text{IR}} \approx 10^{12} L_{\odot}$ . The position of an active source at the center of a  $\sim 50$  kpc-radius ring of linearly polarized Ly $\alpha$  emission detected by Hayes et al. (2011) suggests that the central source is leaking Ly $\alpha$  photons preferentially in the plane of the sky, which undergo scattering in HI clouds at large galactocentric radius. The Ly $\alpha$  morphology around the submillimeter detection is reminiscent of biconical outflow, and the average Ly $\alpha$  line profiles of the two ‘lobes’ are dominated by a red peak, expected for a resonant line emerging from a medium with a bulk velocity gradient that is outflowing relative to the line center. Taken together, these observations provide compelling evidence that the central active galaxy (or galaxies) is responsible for a large fraction of the extended Ly $\alpha$  emission and morphology. Less clear is the history of the cold gas in the circumgalactic medium being traced by Ly $\alpha$ : is it mainly pristine material accreting into the halo that has not yet been processed through an interstellar medium (ISM), now being blown back as it encounters an outflow, or does it mainly comprise gas that has been swept-up within the ISM and expelled from the galaxy?

*Subject headings:* galaxies: active, galaxies: formation, galaxies: high-redshift

## 1. INTRODUCTION: LYMAN- $\alpha$ BLOBS

Lyman- $\alpha$  Blobs (LABs) are  $\sim 100$  kpc scale Lyman- $\alpha$  emission line nebulae, with integrated luminosities up to  $L_{\text{Ly}\alpha} \sim 10^{37}$  W. LABs were first discovered during the course of deep optical narrowband imaging of the Small Selected Area 22<sup>hr</sup> (SSA22) field (Steidel et al. 2000), which was known to contain a significant overdensity of Lyman-break Galaxies

(LBGs) at  $z = 3.09$  (Steidel et al. 1998), although previously Francis et al. (1996) and Keel et al. (1999) had also detected extended Ly $\alpha$  emission around luminous galaxies at  $z = 2.4$  (both in high density environments) and extended Ly $\alpha$  emission was reported to be associated with some of the first high- $z$  submillimetre galaxies (SMGs, e.g., Ivison et al. 1998). Subsequent narrowband (and broadband, see Prescott et al. 2012, 2013) surveys of the SSA22 ‘protocluster’ and elsewhere have since revealed a substantial sample of these high redshift nebulae, with a range of Ly $\alpha$  luminosities and extents (e.g., Matsuda et al. 2004, 2011, Yang et al. 2009, Erb et al. 2011, Bridge et al. 2013).

Since their discovery, the nature of LABs has been in debate. One train of thought is that extended Ly $\alpha$  emission implies the presence of potentially pristine cold gas in the circumgalactic medium (CGM), since low metallicity gas at  $T \sim 10^4$ – $10^5$  K cools most efficiently via Ly $\alpha$  emission through collisional excitation (Fabian & Nulsen 1977, Katz & Gunn 1991, Katz et al. 1996, Haiman et al. 2000). Particular curiosity was aroused because Ly $\alpha$  cooling is a potential observational signature of cold gas streaming into dark matter halos and feeding the discs of young massive galaxies: many cosmological hydrodynamical simulations suggest that the baryonic growth of massive ( $M_h > 10^{12} M_{\odot}$ ) galaxies at  $z > 2$  (and for lower mass galaxies at *all* epochs) is dominated by a mode of ‘cold accretion’ in the form of narrow filamentary streams that penetrate the hot, virially shocked halo gas (Katz et al. 2003, Kereš et al. 2005, 2009, Dekel et al. 2009). It is important to note however that it was recognised that the cooling budget would contain a significant cold component even in the early cold dark matter models (White & Frenk 1991). Despite this, the predicted cold flows have so-far eluded unambiguous observation and indeed, some recent simulations seem to refute the existence of cold flows that survive to the

<sup>1</sup> Center for Astrophysics Research, Science & Technology Research Institute, University of Hertfordshire, Hatfield, AL10 9AB, UK. j.geach@herts.ac.uk

<sup>2</sup> Institute for Computational Cosmology, Department of Physics, Durham University, South Road, Durham, DH1 3LE, UK

<sup>3</sup> Department of Physics & Astronomy, University of Leicester, University Road, Leicester, LE1 7RH, UK

<sup>4</sup> School of Physics, HH Wills Physics Laboratory, Tyndall Avenue, Bristol BS8 1TL, UK

<sup>5</sup> XMM SOC, ESAC, Apartado 78, 28691 Villanueva de la Canada, Madrid, Spain

<sup>6</sup> Department of Physics and Atmospheric Science, Dalhousie University Halifax, NS, B3H 3J5, Canada

<sup>7</sup> Astrophysics Group, Imperial College London, Blackett Laboratory, Prince Consort Road, London, SW7 2AZ, UK

<sup>8</sup> Institute for Astronomy, University of Edinburgh, Royal Observatory, Blackford Hill, Edinburgh EH9 3HJ, UK

<sup>9</sup> Virginia Polytechnic Institute & State University Department of Physics, MC 0435, 910 Drillfield Drive, Blacksburg, VA 24061, USA

<sup>10</sup> Joint Astronomy Centre 660 N. A’ohoku Place University Park Hilo, Hawaii 96720, USA

<sup>11</sup> Department of Astronomy, Cornell University, Ithaca, NY 14853, USA

<sup>12</sup> UK Astronomy Technology Centre, Royal Observatory, Blackford Hill, Edinburgh EH9 3HJ, UK

<sup>13</sup> Department of Physics & Astronomy, University of British Columbia, 6224 Agricultural Road, Vancouver, BC, V6T 1Z1, Canada

<sup>14</sup> Kapteyn Institute, University of Groningen, P.O. Box 800, 9700 AV Groningen, The Netherlands

<sup>15</sup> Leiden Observatory, Leiden University, P.O. box 9513, 2300 RA Leiden, The Netherlands

disc altogether (Nelson et al. 2013). Nevertheless, LABs have been touted as the closest we have come to identifying the filamentary cold mode accretion phenomenon in nature.

While the cosmological gas simulations can track the history of cold gas easily enough, the predicted fluxes of the cooling  $\text{Ly}\alpha$  emission are far more uncertain, with the flux depending on the complex interplay of turbulence, radiative transfer and local sources of ionizing radiation are taken into account (e.g., Rosdahl & Blaiziot 2012). The prescriptions for  $\text{Ly}\alpha$  radiative transfer through the gas are notoriously complex due to the fact that it is a resonant line (Neufeld 1990) and sensitive to assumptions about the sub-grid physics governing the transport of  $\text{Ly}\alpha$  photons through astrophysical media, as well as the many other possible sources of  $\text{Ly}\alpha$  photons in and around galaxies. As a result, different simulations that apply bespoke models of  $\text{Ly}\alpha$  radiative transfer, aiming to reproduce the properties of observed LABs, predict a wide range of physical properties ( $\text{Ly}\alpha$  luminosities can vary by an order of magnitude) and key observables, such as  $\text{Ly}\alpha$  extents and surface brightnesses (Faucher-Giguère et al. 2010, Goerdt et al. 2010, Rosdahl & Blaiziot 2012).

The cold flow picture is complicated further when one considers the effects of the presence of a luminous source (a starburst galaxy or one hosting an active galactic nucleus, AGN) embedded within the LAB, which appears to be a common situation (e.g., Francis et al. 1996, Keel et al. 1999, Dey et al. 2005, Geach et al. 2005, 2007, 2009, Webb 2009, Rauch et al. 2011, Cantalupo, Lilly & Haehnelt 2012). The typical bolometric luminosities of the embedded sources imply an energy balance heavily weighted towards the galaxy, such that only relatively weak coupling, through feedback, would be required to explain the  $\text{Ly}\alpha$  luminosities (Geach et al. 2009). Again, there is further uncertainty in the type of feedback that would give rise to such extended  $\text{Ly}\alpha$  emission: proposals have included emergent (supernovae-driven) superwinds that shock heat cold gas swept up in the outflow (Taniguchi & Shioya 2000), photoionization of the CGM by escaping ultraviolet continuum radiation from massive stars or the accretion discs of an AGN, or photoionization via inverse Compton (IC) scattering of cosmic microwave background (or locally generated far-infrared) photons, which are energetically up-scattered by a relic population of relativistic electrons (e.g., Scharf et al. 2003, Fabian et al. 2009).

Geach et al. (2009) rule-out IC scattering as a viable LAB formation mechanism using a deep X-ray stack in SSA22, arguing that photoionization by a central AGN (which may be present in up to 50% of LABs) is probably more important, even with fairly modest escape fractions likely to be applicable to the often heavily obscured sources. Recently, Hayes et al. (2011) presented evidence that at least some of the extended  $\text{Ly}\alpha$  emission must be in the form of scattered  $\text{Ly}\alpha$  radiation, with  $\text{Ly}\alpha$  photons generated within a central galaxy scattering in clouds of HI at large ( $\sim 50$  kpc) galactocentric radius. The absence of an obvious luminous counterpart in some LABs (e.g., Nilsson et al. 2006, Smith & Jarvis 2007, Smith et al. 2008) has been inferred to be a sign that, in some cases at least, cooling radiation alone is sufficient to explain the extended  $\text{Ly}\alpha$  emission. However, often the constraints on the level of AGN or starburst activity are too poor to rule out the involvement of feedback energy completely.

In practice, it seems likely that a mixture of gravitational cooling and feedback processes are at play in LABs, each imparting an ambiguous observational signature in the  $\text{Ly}\alpha$  emission that is further muddled by observational limitations

(namely angular and spectral resolution, and poor sensitivity to low surface-brightness features). In any case, it is important to note that *both* the cooling and ‘heating’ models require a reasonable reservoir of gas in the circumgalactic medium, so whatever the process dominating the  $\text{Ly}\alpha$  emission, LABs provide a rare opportunity to investigate the astrophysics at the galaxy/intergalactic medium interface close to the formation epoch of massive galaxies,  $z \approx 2-3$ .

## 2. SSA22-LAB1

The archetypal giant LAB, SSA22-LAB1, is the most scrutinized specimen of this class of object, but it is perhaps also the most controversial. Chapman et al. (2001, 2004) reported the detection of a very bright submillimeter galaxy at the center of the nebula, with a  $850\mu\text{m}$  (James Clerk Maxwell Telescope [JCMT]/SCUBA) flux of  $\sim 17$  mJy, implying a galaxy with hyperluminous levels of activity, which Geach et al. (2007) identified with a *Spitzer*-IRAC source likely to be the counterpart. However it appears this measurement over-estimated the submillimeter emission. Matsuda et al. (2007) observed SSA22-LAB1 at higher resolution ( $2''$ ) using the SubMillimeter Array (SMA), at a  $1\sigma$  depth of  $1.4\text{ mJy beam}^{-1}$  at  $880\mu\text{m}$ . The target was not detected, and the conclusion was that the  $850\mu\text{m}$  emission reported by Chapman et al. must be extended on scales of several arcseconds, and resolved out in the SMA map. The mystery deepened when Yang et al. (2012) reported no detection of SSA22-LAB1 at  $870\mu\text{m}$  in an APEX/LABOCA observation, at a similar resolution to the original SCUBA observation (using the on/off chopping technique in photometry mode). The reported  $3\sigma$  upper limit of  $S_{870} < 12$  mJy is clearly at odds with the SCUBA detection. Most recently, in an AzTEC/ASTE  $1.1\text{ mm}$  map of the field, Tamura et al. (2013) report only a marginally significant  $2.7\sigma$  ( $1.9$  mJy) flux enhancement at the position of SSA22-LAB1, again in tension with the original SCUBA observations.

In this paper we present new JCMT/SCUBA-2 observations of SSA22-LAB1, taken as part of the SCUBA-2 Cosmology Legacy Survey (Geach et al. 2013, Roseboom et al. 2013) and interpret the results in the context of extremely deep  $\text{Ly}\alpha$  SAURON integral-field observations (Weijmans et al. 2010) and the recent Very Large Telescope/UV Focal Reducer and low dispersion Spectrograph (FORIS)  $\text{Ly}\alpha$  polarimetry observations of Hayes et al. (2011). The remainder of the paper is organised as follows: in §3 we describe the SCUBA-2 observations, §4 presents the main result and we interpret and discuss this in context with other observations in §5. We conclude the paper with a hypothesis for the origin of SSA22-LAB1, and propose further questions in §6. A  $\Lambda$ CDM cosmology defined by the parameters measured with the *Wilkinson Microwave Anisotropy Probe* (7 year results including baryonic acoustic oscillation and Hubble constant constraints, Komatsu et al. 2011) is assumed throughout:  $h = 0.70$ ,  $\Omega_m = 0.27$ ,  $\Omega_\Lambda = 0.73$ .

## 3. SCUBA-2 OBSERVATIONS

The SSA22 field has been observed as part of the JCMT SCUBA-2 Cosmology Legacy Survey (S2CLS). A  $30$  arcminute diameter map, centered on  $22^{\text{h}}17^{\text{m}}36.3^{\text{s}}$ ,  $+00^{\circ}19'22.7''$ , has been obtained (using multiple repeats of the PONG scanning pattern). A total of 105 observations were made between August 23, 2012 and November 29, 2013 in conditions when the zenith optical depth at  $225\text{ GHz}$  was in the range  $0.05 < \tau_{225} < 0.1$ , with a mean of  $\langle \tau_{225} \rangle = 0.07$ . The

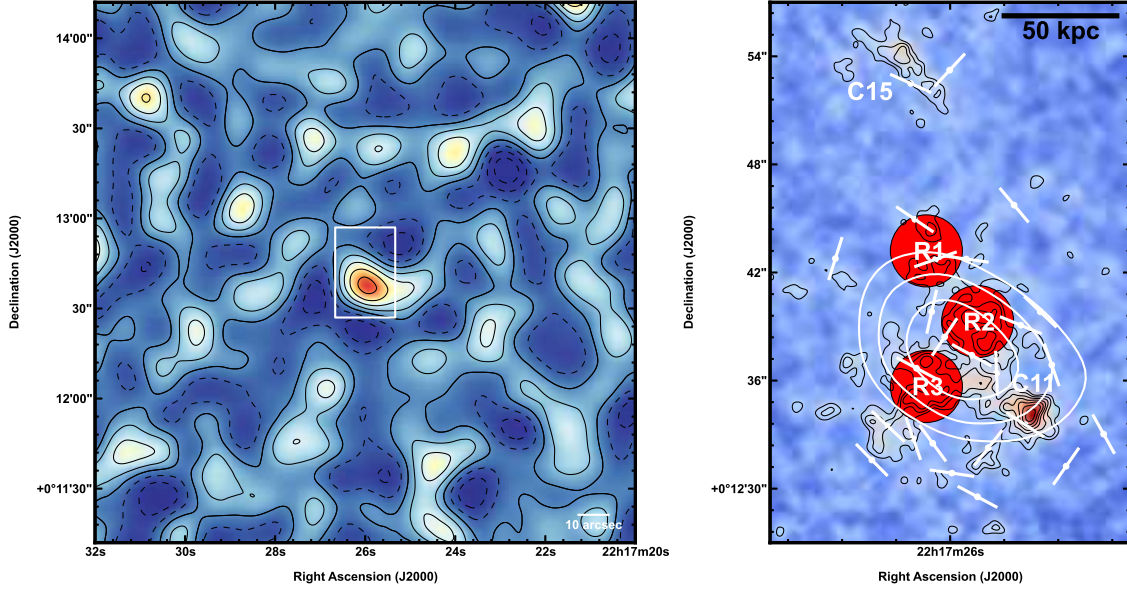


**Figure 1.** (Left) SCUBA-2 850  $\mu\text{m}$  map of the region ( $3' \times 3'$ ) around SSA22-LAB1; contours indicate significance levels of  $-5 \leq \sigma \leq 5$  in steps of  $1\sigma$ , where  $1\sigma = 1.1 \text{ mJy beam}^{-1}$ . We detect a source with  $S_{850} = (4.6 \pm 1.1) \text{ mJy beam}^{-1}$  at the position of SSA22-LAB1, and confirm that a  $\sim 3\sigma$  detection is measured at the same position in independent halves of the data (§4). The white box shows the SAURON field of view, detailed in the second panel. (Right) zoom-in of SSA22-LAB1 showing the average line flux over 4922–5022 Å observed in a 24 hour integration with the SAURON IFU (Matsuda et al. 2004, Weijmans et al. 2010). We show the SCUBA-2 detection as contours ( $0.5\sigma$  levels starting at  $3\sigma$ ). The LAB clearly breaks up into distinct regions, two of which are centered on Lyman-break galaxies (C11 and C15) at  $z = 3.1$ , whereas R1-R3 are more diffuse and not obviously connected with an ultraviolet continuum source. White lines show the direction of the polarization pseudovectors ( $\chi = 0.5 \arctan(U/Q)$ , where  $U$  and  $Q$  are the Stokes parameters, Hayes et al. 2011). The polarization pattern describes a ring surrounding the SMG, and we postulate that this is the source of Ly $\alpha$  photons, which are escaping the galaxy and scattering in H I clouds at large radius.

beam-convolved map reaches a  $1\sigma$  depth of  $1.1 \text{ mJy beam}^{-1}$  with an integration time of  $\sim 3000$  seconds per 4 arcsecond pixel. Data are reduced using the SMURF *makemap* pipeline (Chapin et al. 2013), following the procedures described in more detail in Geach et al. (2013). Flux calibration is performed using the best estimate of the flux conversion factor based on observations of hundreds of standard calibrators (Dempsey et al. 2013); this absolute flux calibration is expected to be accurate at the 15% level.

#### 4. RESULTS

A submillimeter source with  $S_{850} = (4.6 \pm 1.1) \text{ mJy}$  (error bar is instrumental noise only) is detected at  $22^{\text{h}}17^{\text{m}}26.0^{\text{s}}$ ,  $+00^{\circ}12'37.5''$ . This is within  $1.5''$  of a red *Spitzer*-IRAC continuum counterpart source ( $S_8 = 7.6 \pm 2.2 \mu\text{Jy}$ ,  $S_8/S_{4.5} = 1.3 \pm 2.2$ ), close to the center of the Ly $\alpha$  halo that Geach et al. (2007) identified as the central galaxy. To investigate the veracity of the submillimeter detection, we create two ‘half maps’ from the SCUBA-2 data, whereby each half map represents a random 50% of the individual scans used to make the total map. At the sky position of the detection reported above, we measure significant flux densities of  $(4.8 \pm 1.6) \text{ mJy}$  and  $(4.5 \pm 1.5) \text{ mJy}$  (i.e.,  $3\sigma$  detections with consistent flux densities in independent halves of the integration), which lend credence to the submillimeter detection of SSA22-LAB1.

Chapman et al. (2004) also present a tentative VLA 1.4 GHz radio continuum source and Owens Valley Radio Observatory (OVRO) CO(4–3) detection consistent with this position (although Yang et al. 2012 failed to detect CO(4–3) in SSA22-LAB1 with IRAM PdBI). The SCUBA-2 map in the vicinity of SSA22-LAB1 is shown in Fig. 1. The mid-infrared colours of the IRAC counterpart suggest that star formation dominates the energy budget of this source (Colbert et al. 2011). Clearly the new 850  $\mu\text{m}$  flux density is lower than the

$S_{850} = 16.8 \pm 2.9 \text{ mJy}$  reported by Chapman et al. (2001), but it is worth noting that formally the flux density ratio of the initial SCUBA measurement and the new SCUBA-2 flux density is  $3.7 \pm 1.1$ ; effects such as flux boosting could well have elevated the observed flux density in the original SCUBA data.

The revised 850  $\mu\text{m}$  flux density is consistent with the LABOCA upper-limit  $S_{870} < 12 \text{ mJy}$  (Yang et al. 2012), and at the  $1\sigma$   $1.4 \text{ mJy beam}^{-1}$  limit of the higher-resolution ( $2''$  beam) SMA map of Matsuda et al. (2007), the 850  $\mu\text{m}$  emission would only have to be distributed on a scale of a few arcseconds to fall below the SMA detection rate. Still, the galaxy-integrated 850  $\mu\text{m}$  emission implies a vigorously star-forming galaxy. With no other constraints on the shape of the far-infrared spectral energy distribution, we can only make a rough estimate of the bolometric (total infrared) luminosity. Assuming a nominal single modified blackbody spectrum with  $\beta = 2$  and  $T = 20\text{--}30 \text{ K}$  (Magnelli et al. 2012), normalised to  $S_{850} = 4.6 \text{ mJy}$  (the data do not allow a constraint on either the emissivity or temperature), implies a  $\log(L_{\text{IR}}/L_{\odot}) \approx 11.8\text{--}12.6$ , where the infrared luminosity is integrated over  $\lambda = 40\text{--}120 \mu\text{m}$  (rest frame) and includes a bolometric correction term of 1.91 to account for hot dust emission at mid-infrared wavelengths not modelled by the single blackbody (Helou et al. 1988; Dale et al. 2001; Magnelli et al. 2012).

The integrated luminosity estimated above should be considered with a caveat: the  $15''$  resolution of the SCUBA-2 map naturally results in a submillimeter flux measurement that is integrated over the equivalent of  $\sim 120 \text{ kpc}$  at  $z = 3.1$ , thus encompassing (potentially) several individual sources contributing to the 850  $\mu\text{m}$  emission. It is already well known that a significant fraction of submillimeter galaxies ( $\sim 35\%$  and potentially up to  $50\%$ ) detected with coarse resolution instruments break-up into several components when observed at higher resolution, as is now possible with sensitive inter-

ferometers (e.g., Hodge et al. 2013). Given the negative  $k$ -correction in the submillimeter bands on the Rayleigh-Jeans side of the cool dust emission, chance alignments of luminous galaxies across a wide range of epochs could give rise to multiplicity, however, given the likelihood that many high- $z$  submillimeter sources are either physically large, clumpy systems or undergoing mergers means that single detections that resolve into multiple components does not preclude them being considered part of the same physical system. Obviously obtaining higher resolution submillimeter continuum imaging of SSA22-LAB1 is now a goal, since that will address this question.

There are some hints that we might expect the SCUBA-2  $850\ \mu\text{m}$  detection to be extended: the failure to detect continuum emission in the  $2''$  resolution SMA map of Matsuda et al. (2007) with a  $3\sigma$  upper limit of  $4.2\ \text{mJy beam}^{-1}$  suggests that the  $850\ \mu\text{m}$  flux is distributed on a scale of at least  $>2''$ . At the position of the IRAC counterpart, SSA22-LAB1a identified by Geach et al. (2007), an *HST*-STIS image reveals several distinct (but extremely faint) ultraviolet components spread over several arcseconds (Chapman et al. 2004). For the sake of argument, in the following we will refer to the central source as a single ULIRG-class galaxy (since, even if the emission was distributed on scales of several arcseconds, this is far smaller than the  $\text{Ly}\alpha$  extent of the LAB), but the reader should remember that at all times we are referring to the total infrared luminosity sampled by the JCMT beam, and this could encompass several distinct – but physically associated – sources.

## 5. INTERPRETATION AND DISCUSSION

The detection of a luminous galaxy in the core of SSA22-LAB1 is further evidence that Lyman- $\alpha$  Blobs are generally associated with luminous young galaxies, be it an obscured starburst or an AGN (Geach et al. 2009). SSA22-LAB1 is unique in that it has been studied in far greater detail than any other LAB, and therefore offers the best opportunity to understand the astrophysics of the LAB phenomenon.

### 5.1. Spatial distribution and spectral properties of the Lyman- $\alpha$ emission

Weijmans et al. (2010) present very deep WHT/SAURON integral field unit (IFU) spectral observations of SSA22-LAB01 at  $4810\text{\AA} < \lambda < 5350\text{\AA}$ , combining the data with the previous observations of Bower et al. (2004) to form a data cube with total integration time of nearly 24 hours. The IFU data provide a much better probe of the structure of the  $\text{Ly}\alpha$  halo than narrow-band imaging alone (Steidel et al. 2000, Matsuda et al. 2004).

One of the main findings of the SAURON survey was the discovery that the nebula clearly breaks up into several distinct emission regions, which we show in Fig. 1. At the southern and northern extent of the structure, extended  $\text{Ly}\alpha$  emission is associated with two  $z = 3.09$  Lyman Break Galaxies (C11 and C15, Steidel et al. 1998, 2000)<sup>16</sup>. As originally pointed out by Bower et al. (2004), C11 and C15 exhibit strong velocity shear in their extended  $\text{Ly}\alpha$  emission, which, in the case of C15 at least, is likely to be indicative of an outflow, given that the orientation of the shear is approximately

normal with respect to the major axis of the galaxy, revealed in *HST*/STIS imaging (Weijmans et al. 2010).

There are three other main regions of  $\text{Ly}\alpha$  emission, labelled R1, R2 and R3 by Weijmans et al. These contain no ultraviolet continuum source, but the two brightest components R2 and R3 ( $L_{\text{Ly}\alpha} = 2.3 \times 10^{36}\ \text{W}$  and  $2.7 \times 10^{36}\ \text{W}$  respectively) approximately straddle the peak of the  $850\ \mu\text{m}$  emission. R1 is best described as a lower surface brightness filament extending north from R2 towards C15. In Fig. 2 we present the average  $\text{Ly}\alpha$  spectra extracted from  $2''$  radius apertures at the positions R1, R2 and R3 indicated on Fig. 1. All the lines are broad, with FWZI widths of  $\sim 400\ \text{km s}^{-1}$ , and poorly fit by single Gaussian dispersion profiles. As Weijmans et al. show, a double Gaussian fit is a better model of the line profiles in all three cases (a single Gaussian combined with a Voigt absorption profile also provides an adequate fit to the data). In Fig. 2 we show the best fitting double Gaussian profiles, where we have taken into account the instrumental dispersion ( $108\ \text{km s}^{-1}$ ), and centered in the rest frame of each component. R2 and R3 are within  $180\ \text{km s}^{-1}$  of each other, and both profiles have a dominant red-skewed peak. In contrast, R1 has a slightly more prominent blue peak and is separated from R2 by approximately  $300\ \text{km s}^{-1}$ .

The  $\text{Ly}\alpha$  line profile is sensitive to the complexities of the radiative transfer physics of a resonant line (e.g., Neufeld 1990). For resonant line radiation transfer through an optically thick slab the emergent line profile is symmetric and double peaked, with a minimum at  $\Delta v = 0$  due to scattering at the line resonance (Neufeld 1990). In an HI cloud, the separation of the peaks is set by the gas temperature and column density, which determine the typical frequency change a photon can experience through scattering. If a large-scale velocity gradient is present, then the line profile becomes asymmetric, with either the red or blue peak dominating, depending on the direction of the velocity gradient with respect to the resonant frequency: outflows generally result in a prominent red peak, whereas infall results in a dominant blue peak ( $z < z_{\text{em}}$   $\text{Ly}\alpha$  Forest absorption suppresses the blue wing whatever the situation). Turbulent motions within the medium will also broaden the emergent line.

Asymmetric line profiles can also occur due to foreground absorption of  $\text{Ly}\alpha$  photons by clumps, or screens, of dust or HI (as is proposed for the line profile observed in LAB2, see Wilman et al. 2005). With this in mind, and considering the complexities of the  $\text{Ly}\alpha$  radiative transfer, not to mention the limitations of current instrumentation (for example spectral resolution), interpretation is often ambiguous. However, it is interesting that the line profiles of R2 and R3 both have dominant red peaks; given their spatial distribution relative to the SMG, one could interpret this as evidence of a biconical outflow driven by the central ULIRG. Photons from the central source that are back-scattered from the interior, rear wall of the expanding shell will be redshifted out of resonance with the front wall, while photons forward scattered from the front wall remain in resonance with the expanding shell. Note, that the bipolar appearance does not necessarily require that the outflow is bipolar. The emergent structure could be equally well explained if ionizing photons only escaped from the central source along preferential directions.

More tantalising, perhaps, is the slightly blue-skewed line profile of the more filamentary (and fainter) R1 emission extending north from R2 and pointing towards C15: could this be evidence of an inflowing stream? Given that (a) inflows of

<sup>16</sup> The extended emission around C15 was actually classified as a separate LAB (SSA22-LAB08) by Matsuda et al. (2004), who based LAB identification on isophotal threshold, although the proximity of C15 to the main bulk of SSA22-LAB1, and the faint filament of  $\text{Ly}\alpha$  emission connecting them suggests we should consider C15 as part of the SSA22-LAB1 system proper.

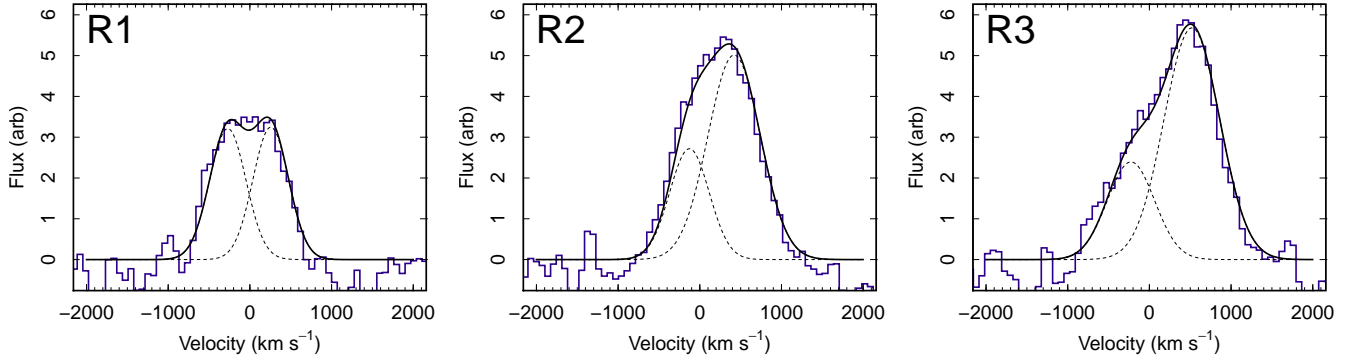


**Figure 2.** Average Ly $\alpha$  line profiles extracted from the  $4''$ -diameter apertures R1–R3 indicated in Fig. 1, shown on a common, but arbitrary, flux scale. R1 is a low surface brightness filamentary structure extending north from R2 towards the LBG C15, whereas the brighter R2 and R3 represent two ‘lobes’ of emission straddling the SMG. The lines are all broad and asymmetric, with R2 and R3 showing prominent red peaks, expected if a bulk velocity gradient is present that is positive relative to the line center, and usually interpreted as outflowing material. The profile of the R1 spur, in contrast, is more symmetric, and it is unclear whether this gas is inflowing, outflowing or static relative to the central galaxy.

cold gas in massive haloes are now established as an important feature of galaxy formation models, and that (b) the intense phases of galaxy growth (starbursts and supermassive black hole growth) giving rise to powerful outflows are expected to be co-eval with gas inflow, we should not be surprised to see both processes in action in the same system.

### 5.2. Polarized Lyman- $\alpha$ emission: scattering of photons from a central ULIRG?

Hayes et al. (2011) used VLT/FORS to measure the polarization of the extended Ly $\alpha$  emission in SSA22-LAB1. In Fig. 1 we overlay the polarization pseudovectors ( $\chi$ ), where  $\chi = 0.5 \arctan(U/Q)$  and  $U$  and  $Q$  are the Stokes parameters. Note the ring-like geometry of the polarization vectors at large radii, centered approximately at the position of the SMG, and generally tracing components R2 and R3. The polarization fraction  $P$  reaches approximately 20% at a radius of 45 kpc. A ring of polarized Ly $\alpha$  emission observed at large radii from the geometric center of the LAB cannot be generated *in situ*, but is more likely to be scattered light originating from a central source. In this model, Ly $\alpha$  photons escaping from a star-forming galaxy or AGN undergo a long flight, before encountering H I clouds in the CGM and scattering. A geometry where the photon–atom vector angle is  $90^\circ$  prior to scattering imparts the greatest polarization signal.

As Hayes et al. explain, it is the rare wing scatterings (i.e. photons with large  $\Delta\nu$  from the Ly $\alpha$  line center in the rest frame of an H I cloud) that (a) see lower optical depth and are more likely to escape the neutral gas-filled halo and (b) have a higher probability of becoming polarized, with a polarization fraction up to  $P \sim 40\%$ . This is compared to more numerous ‘core scatterings’ which are not only less likely to be polarized ( $P < 7\%$ ), but also less likely to escape to the line of sight. For these reasons, neither shock excitation, photoionization or collisional excitation during gravitational cooling in the in-flowing streams can explain the polarization observations, although this is not to say the total Ly $\alpha$  luminosity is not contributed to in part by non-scattering processes.

The detection of an SMG with  $L_{\text{IR}} \sim 10^{12} L_\odot$  located between the lobes of R2 and R3 is a smoking gun: not only is the SMG spatially coincident with the center of the polarization pattern, but its bolometric luminosity, presumably dominated by far-infrared emission, indicates an ample supply of Ly $\alpha$

photons, even if the majority of these are absorbed by interstellar dust. Considering a naive model where the infrared luminosity is produced entirely from re-processed starlight and represents the bulk of the active star formation, we expect an *intrinsic* Ly $\alpha$  luminosity of order  $L_{\text{Ly}\alpha}^{\text{int}} \approx 0.05 L_{\text{IR}}$  for Case B recombination and a Salpeter initial mass function (Kennicutt et al. 1998, Dijkstra & Westra 2009). Thus, the escaping Ly $\alpha$  luminosity is  $L_{\text{Ly}\alpha}^{\text{esc}} \approx 0.05 f_{\text{esc}} L_{\text{IR}}$ , where  $f_{\text{esc}}$  is the escape fraction of Ly $\alpha$  photons from the central galaxy. However, only a fraction,  $f_{\text{scat}}$ , of these Ly $\alpha$  photons will go on to scatter in the CGM into our line of sight and thus give rise to the LAB.

Three key factors affect  $f_{\text{scat}}$ : (i) the cross-section for Ly $\alpha$ –H I scattering for photons encountering surrounding neutral gas; (ii) the overall filling factor of those clouds around the central source and; (iii) the velocity distribution of the neutral gas determining how photons can move out of resonance and free stream to the observer. Clearly (i) is dependent on the  $N_{\text{H}}$  column, but since  $f_{\text{scat}} < 1$  even for filling factors of unity, this increases the escape fraction required from the central source if scattered light is the sole source of extended Ly $\alpha$  emission. For  $L_{\text{IR}} = 10^{12} L_\odot$ , this requires  $f_{\text{esc}} > 25\%$  to account for the total  $L_{\text{Ly}\alpha}$  of R2 and R3. This is not unreasonable if one considers a geometry where we are viewing the ULIRG system nearly edge-on, with a large optical depth to the star-forming regions and thus any ultraviolet continuum emission from the central source completely obscured along our line of sight but instead escaping in the plane of the sky (see Geach et al. 2007). This geometry would also impart the largest observable Ly $\alpha$  polarization signal, as photons escaping to our line of sight would be scattered through  $90^\circ$ , and would produce a morphology consistent with the double lobed Ly $\alpha$  geometry hinted at by the deep SAURON observations described above.

## 6. CONCLUSIONS

### 6.1. A model of LAB formation: a combination of velvet rope and bouncer feedback?

The observations imply that one of the main sources of Ly $\alpha$  photons emitted by SSA22-LAB1 is either star formation or an AGN within the embedded ULIRG. These photons are escaping the galaxy and scattering in cold gas distributed in the CGM. Whatever the exact mechanism for Ly $\alpha$  emission, there must be a large quantity of cold, neutral gas in the CGM. An



open question therefore is the origin of the circumgalactic gas responsible for scattering/emitting the Ly $\alpha$  photons and giving rise to the observed extended emission-line nebula. There are two options:

1. The cold gas is comprised of pristine material containing dense clumps of HI being accreted onto the dark matter halo (Zheng et al. 2011), potentially delivered by narrow streams within a hotter medium. Ly $\alpha$  photons escaping the central galaxy illuminate this gas as they scatter in the clumpy, neutral medium. The morphology of the resulting LAB is therefore somewhat dependent on the geometry of the escaping photons and the covering factor of the incoming clumps, which could be modified as the inflow encounters radiation/outflows from the galaxy.
2. Neutral gas is being ejected into the CGM via a galactic outflow, having already been accreted onto the galaxy. The outflow forms when shells of cold gas are driven outwards by pressurized bubbles inflated within the ISM via energy/momentum injection from stellar winds, supernovae and AGN. The outflow strongly resembles a rarefaction wave escaping the galaxy along paths of least resistance (e.g., perpendicular to the disc), accelerating as they emerge into the low-pressure CGM before fragmenting into cold clumps due to hydrodynamic instabilities and eventually decelerating in the gravitational potential of the halo (Dijkstra & Kramer 2012, Creasey et al. 2013).

The key difference between (1) and (2) is the provenance and history of the cold gas dominating the CGM: pristine still-cooling or previously cycled through a galaxy? The two scenarios describing the history of the CGM can be related to the concept of ‘velvet rope’ and ‘bouncer’ feedback<sup>17</sup>. In velvet rope feedback, gas never gets a chance to enter a galaxy where it can be assimilated into the ISM. In contrast, bouncer mode describes feedback that ejects gas from the galaxy back into the CGM.

Of course, these scenarios are not mutually exclusive. Gas must be delivered to growing galaxies at some point, and this is likely to be close to, or simultaneous with, the time the galaxies undergo their most rapid growth. Therefore it is possible that emergent shells comprised of enriched gas could also sweep-up cold, metal-free inflowing material that has not yet reached the disc (thus, potentially preventing it from being accreted: velvet rope feedback). In scenario 1, some of the inflowing gas might be being blown back by an emergent wind, and the observations suggest that the bulk of the line-emitting gas is outflowing with respect to the central ULIRG (Fig. 2). One problem with this scenario is that the covering factors of the streams are expected to be very small, of order a few per cent (Faucher-Giguère & Kereš 2011). Outflows are likely to emerge preferentially between these streams, allowing the cold inflowing material to continue to fuel the disc unabated, while cold interstellar material is simultaneously ejected (bouncer feedback). However, the interaction of multi-phase galactic outflows and the narrow cooling streams predicted by models is poorly understood, the hydrodynamic interaction between the two is likely to be complicated, dependent on halo mass, geometry and radius. Moreover, the

halo will still have a diffuse atmosphere, even if most of the mass is accreted along filamentary structure (e.g., Crain et al. 2013).

While the cold flows model predicts that the inflowing cold gas should also be a source of Ly $\alpha$  radiation from collisional excitation, the polarization observations show that a significant fraction of the Ly $\alpha$  emission is not produced *in situ*. However, in a scenario where Ly $\alpha$  photons from the central source are scattering in HI clumps in these streams, one must consider the small covering factors predicted for the inflowing cold filaments ( $f \sim 1\text{--}3$  per cent; Faucher-Giguère & Kereš 2011). If the escaping Ly $\alpha$  photons are uncorrelated with the geometry of the filaments (which could be a naive assumption if one considers that the escape must preferentially be in the directions of lowest density, i.e., potentially *anti*-correlated with the filaments), then one would expect a fraction  $(1 - f)$  of the Ly $\alpha$  photons *not* to scatter. In effect, this drastically increases the required Ly $\alpha$  luminosity of the central source. In contrast, gas entrained in a galaxy-scale wind can have covering factors approaching unity, which arguably would result in an observed Ly $\alpha$  morphology similar to R2 and R3.

Francis et al. (2013) argue that the CGM of Ly $\alpha$  Blob B1 ( $z = 2.38$ ) could also be illuminated by scattered Ly $\alpha$  radiation, either originating from a central source, or via fast shocks in the CGM. In the superwind scenario, the fast shock is formed when hot gas driven by the emergent wind from the central source collides with cold gas in the CGM. The detection of C IV in the CGM of B1 is taken to be evidence for gas heating via fast shocks (Francis et al. 2001), and Francis et al. (2013) argue that the presence of carbon rules out a primordial origin for this material. Enriched cold gas in the vicinity of low-mass satellites within the halo could be the origin (these could also contribute Ly $\alpha$  luminosity via ultraviolet leakage), as could metal-rich gas previously ejected from the central source. Still, a primordial origin for at least a fraction of the cold gas cannot be ruled out, and indeed should be expected.

## 6.2. Final comments

It seems that a coherent picture for the SSA22-LAB1 system is at last emerging, although puzzles still remain. The SSA22-LAB1 system is clearly a group in the early stage of formation, and while the Ly $\alpha$  ‘bridge’ linking the northern LBG C11 with the main emission structure may well be a remnant cooling flow, the evidence suggests that a significant fraction of the Ly $\alpha$  emission originates in the central ULIRG and scatters in HI clouds distributed in the CGM. The twist is that the central source does not emit Ly $\alpha$  photons isotropically, indeed, we do not see ionizing photons from the source, let alone the escaping Ly $\alpha$  radiation. Nevertheless, the new SCUBA-2 observations presented here allow us to observe the ultraviolet photons that are reprocessed by internal dust along our line-of-sight. Although we do not see the ultraviolet continuum source directly, abundant Ly $\alpha$  photons (and presumably a strong flux of ionizing photons) must escape along an axis that is almost perpendicular to the line of sight. Viewed along the emergent axis from another part of the Universe we would almost certainly identify the source as a Ly $\alpha$  halo containing an ultraviolet continuum source.

SSA22-LAB1 offers a fascinating insight into the physics of massive galaxy formation: many of the ingredients of our latest models appear to be in action in this one system, and it clearly provides a unique opportunity to study the astrophysics of the galaxy/CGM interface. There are three key observations that would provide more important clues:

<sup>17</sup> terms attributed to N. Katz

1. Sensitive, high-resolution Ly $\alpha$  imaging. This would more clearly reveal the morphology of the cold circumgalactic gas as traced by Ly $\alpha$ , providing the finer detail that might help distinguish an outflow with large covering factor from narrow filamentary streams. SSA22-LAB1 is an ideal target for the Multi Unit Spectroscopic Explorer (MUSE) IFU being commissioned on the Very Large Telescope.
2. Morphology of the dust continuum. High resolution sub-mm imaging would more accurately pin-point the ULIRG within the Ly $\alpha$  halo and potentially provide a clearer picture of the nature of the central luminous source, including the geometry of the obscuring material.
3. Systemic redshift of the ULIRG. If the galaxy is responsible for a biconical outflow in the plane of the sky (as suggested by the relative velocities of the regions R2 and R3), then it should be very close in redshift space to the Ly $\alpha$  peaks of R2 and R3. The ULIRG systemic redshift could be measured with millimetre observations of high- $J$  CO lines, which should trace the densest molecular gas at the sites of star formation within the ULIRG, and thus provide an accurate measurement of the systemic redshift relative to the extended Ly $\alpha$ .

## ACKNOWLEDGEMENTS

We thank Matthew Hayes for providing the polarization data shown in Figure 1, and for helpful discussions, Anne-Marie Weijmans for providing the SAURON data cube and Rob Crain, Mark Dijkstra, and Claude-André Faucher-Giguère for useful discussions. J.E.G. acknowledges support from the Royal Society by way of a University Research Fellowship. J.S.D. acknowledges the support of the European Research Council via an Advanced Grant, and the contribution of the EC FP7 SPACE project ASTRODEEP (Ref.No: 312725). The James Clerk Maxwell Telescope is operated by the Joint Astronomy center on behalf of the Science and Technology Facilities Council of the United Kingdom, the National Research Council of Canada, and (until 31 March 2013) the Netherlands Organisation for Scientific Research. Additional funds for the construction of SCUBA-2 were provided by the Canada Foundation for Innovation.

## REFERENCES

- Bower, R. G., Morris, S. L., Bacon, R., Wilman, R. J., Sullivan, M., Chapman, S., Davies, R. L., de Zeeuw, P. T., Emsellem, E., 2004, MNRAS, 351, 63
- Bridge, C. R., et al., 2013, ApJ, 769, 91
- Cantalupo, S., Lilly, S. J., Haehnelt, M. G., 2012, MNRAS, 425, 1992
- Chapin, E. L., Berry, D. S., Gibb, A. G., Jenness, T., Scott, D., Tilanus, R. P. J., Economou, F., Holland, W. S., 2013, MNRAS, 430, 2545
- Chapman, S. C., Lewis, G. F., Scott, D., Richards, E., Borys, C., Steidel, C. C., Adelberger, K. L., Shapley, A. E., 2001, ApJ, 548, L17
- Chapman, S. C., Scott, D., Windhorst, R. A., Frayer, D. T., Borys, C., Lewis, G. F., Ivison, R. J., 2004, ApJ, 606, 85
- Colbert, J. W., Scarlata, C., Teplitz, H., Francis, P., Palunas, P., Williger, G. M., Woodgate, B., 2011, ApJ, 728, 59
- Crain, R. A., McCarthy, I. G., Schaye, J., Theuns, T., Frenk, C. S., 2013, MNRAS, 432, 3005
- Creasey, P., Theuns, T., Bower, R. G., 2013, MNRAS, 429, 1922
- Dale, D. A., Helou, G., Contursi, A., Silbermann, N. A., Kolhatkar, S. 2001, ApJ, 549, 215
- Dekel, A., Birnboim, Y., Engel, G., Freundlich, J., Goerdt, T., Mucic, M., Neistein, E., Pichon, C., Teyssier, R., Zinger, E., 2009, Nature, 457, 451
- Dempsey, J. T., et al., 2013, MNRAS, 430, 2534
- Dey, A., et al., ApJ, 629, 654
- Dijkstra, M., Westra, E., 2010, MNRAS, 401, 2343
- Dijkstra, M., Kramer, R., 2012, MNRAS, 424, 1672
- Erb, D. K., Bogosavljević, M., Steidel, C. C., 2011, ApJ, 740, L31
- Fabian, A. C., Nulsen, P. E. J., 1977, MNRAS, 180, 479
- Fabian, A. C., Chapman, S., Casey, C. M., Bauer, F., Blundell, K. M., 2009, MNRAS, 395, L67
- Faucher-Giguère, C.-A., Kereš, D., Dijkstra, M., Hernquist, L., Zaldarriaga, M., 2010, ApJ, 725, 633
- Faucher-Giguère, C.-A., Kereš, D., 2011, MNRAS, 412, L118
- Francis, P. J., et al. 1996, ApJ, 457, 490
- Francis, P. J., et al., 2001, ApJ, 554, 1001
- Francis, P. J., Dopita, M. A., Colbert, J. W., Palunas, P., Scarlata, C., Teplitz, H., Williger, G. M., Woodgate, B. E., 2013, MNRAS, 428, 28
- Geach, J. E., et al., 2005, MNRAS, 363, 1398
- Geach, J. E., Smail, I., Chapman, S. C., Alexander, D. M., Blain, A. W., Stott, J. P., Ivison, R. J., 2007, ApJ, 655, L9
- Geach, J. E., et al., 2009, ApJ, 700, 1
- Geach, J. E., et al., 2013, MNRAS, 432, 53
- Goerdt, T., Dekel, A., Sternberg, A., Ceverino, D., Teyssier, R., Primack, J. R., 2010, MNRAS, 407, 613
- Haiman, Z., Spaans, M., Quataert, E., 2000, ApJ, 537, L5
- Hayes, M., Scarlata, C.; Siana, B. D., 2011, Nature, 476, 304
- Helou, G., Khan, I. R., Malek, L., Boehmer, L. 1988, ApJS, 68, 151
- Katz, N., Gunn, J. E., 1991, ApJ, 377, 365
- Katz, N., Weinberg, D. H., Hernquist, L., 1996, ApJS, 105, 19
- Katz, N., Kereš, D., Dusan, Davé, R., Weinberg, D. H., 2003, The IGM/Galaxy Connection: The Distribution of Baryons at  $z=0$ , ASSL Conference Proceedings Vol. 281. Edited by Jessica L. Rosenberg and Mary E. Putman. ISBN: 1-4020-1289-6, Kluwer Academic Publishers, Dordrecht, 2003, p.185
- Keel, W. C., Cohen, S. H., Windhorst, R. A., Waddington, I., 1999, AJ, 118, 2547
- Kennicutt, R. C. Jr, 1998, ARA&A, 36, 189
- Kereš, D., Katz, N., Weinberg, D. H., Davé, R., 2005, MNRAS, 363, 2
- Kereš, D., Katz, N., Fardal, M., Davé, R., Weinberg, D. H., 2009, MNRAS, 395, 160
- Komatsu, E., et al., 2011, ApJS, 192, 18
- Magnelli, B., et al., et al., 2012, A&A, 539, A155
- Matsuda, Y., et al., 2004, AJ, 128, 569
- Matsuda, Y., Iono, D., Ohta, K., Yamada, T., Kawabe, R., Hayashino, T., Peck, A. B., Petitpas, G. R., 2007, ApJ, 667, 667
- Matsuda, Y., et al., 2011, MNRAS, 410, L13
- Nelson, D., Vogelsberger, M., Genel, S., Sijacki, D., Kereš, D., Springel, V., Hernquist, L., 2013, MNRAS, 429, 3353
- Neufeld, D. A., 1990, ApJ, 350, 216
- Nilsson, K., K., Fynbo, J. P. U., Møller, P., Sommer-Larsen, J., Ledoux, C., 2006, A&A, 452, L23
- Prescott, M. K. M., Dey, A., Jannuzi, B. T., 2012, ApJ, 748, 125
- Prescott, M. K. M., Dey, A., Jannuzi, B. T., 2013, ApJ, 762, 38
- Rauch, M., Becker, G. D., Haehnelt, M. G., Gauthier, J.-R., Ravindranath, S., Sargent, W. L. W., 2011, MNRAS, 418, 1115
- Rosdahl, J., Blaizot, J., 2012, MNRAS, 423, 344
- Roseboom, I. G., 2013, MNRAS, 436, 430
- Scharf, C., Smail, I., Ivison, R., Bower, R., van Breugel, W., Reuland, M., 2003, ApJ, 596, 105
- Smith, D. J. B., Jarvis, M. J., 2007, MNRAS, 378, L49
- Smith, D. J. B., Jarvis, M. J., Lacy, M., Martínez-Sansigre, A., 2008, MNRAS, 378, L49
- Steidel, C. C., Adelberger, K. L., Shapley, A. E., Pettini, M., Dickinson, M., Giavalisco, M., 2000, ApJ, 532, 170
- Steidel, C. C., Adelberger, K. L., Dickinson, M., Giavalisco, M., Pettini, M., Kellogg, M., 1998, ApJ, 492, 428
- Tamura, Y., et al., 2013, MNRAS, 430, 2768
- Taniguchi, Y., Shioya, Y., 2000, ApJ, 532, L13
- Webb, T. M. A., Yamada, T., Huang, J.-S., Ashby, M. L. N., Matsuda, Y., Egami, E., Gonzalez, M., Hayashino, T., 2009, ApJ, 692, 1561
- White, S. D. M., Frenk, C. S., 1991, ApJ, 379, 52
- Weijmans, A.-M., Bower, R. G., Geach, J. E., Swinbank, A. M., Wilman, R. J., de Zeeuw, P. T., Morris, S. L., 2010, MNRAS, 402, 2245
- Wilman, R. J., Gerssen, J., Bower, R. G., Morris, S. L., Bacon, R., de Zeeuw, P. T., Davies, R. L., 2005, Nature, 436, 227
- Yang, Y., Zabludoff, A., Tremonti, C., Eisenstein, D., Davé, R., 2009, ApJ, 693, 1579
- Yang, Y., et al., 2012, ApJ, 744, 178

Zheng, Z., Cen, R., Weinberg, D., Trac, H., Miralda-Escudé, J., 2011, ApJ,  
739 L39